

Aerosol optical depth increase in partly cloudy conditions

Duli Chand,¹ Robert Wood,² Steven J. Ghan,¹ Minghui Wang,¹ Mikhail Ovchinnikov,¹ Philip J. Rasch,¹ Steven Miller,³ Bret Schichtel,⁴ and Tom Moore⁵

Received 5 April 2012; revised 26 July 2012; accepted 3 August 2012; published 14 September 2012.

[1] Remote sensing observations of aerosol from surface and satellite instruments are extensively used for atmospheric and climate research. From passive sensors, the apparent cloud-free atmosphere in the vicinity of clouds often appears to be brighter than further away from the clouds, leading to an increase in the retrieved aerosol optical depth (τ). Mechanisms contributing to this enhancement or increase, including contamination by undetected clouds, hygroscopic growth of aerosol particles, and meteorological conditions, have been debated in recent literature, but the extent to which each of these factors influence the observed enhancement ($\Delta\tau$) is poorly known. Here we used 11 years of daily global observations at $10 \times 10 \text{ km}^2$ resolution from the MODIS on the NASA Terra satellite to quantify τ as a function of cloud fraction (CF). Our analysis reveals that, averaged over the globe, the clear sky τ is enhanced by $\Delta\tau = 0.05$ in cloudy conditions (CF = 0.8–0.9). This enhancement in $\Delta\tau$ corresponds to relative enhancement of 25% in cloudy conditions (CF = 0.8–0.9) compared with relatively clear conditions (CF = 0.1–0.2). Unlike the absolute enhancement $\Delta\tau$, the relative increase in τ is rather consistent in all seasons and is 25–35% in the subtropics and 15–25% at mid and higher latitudes. Using a simple Gaussian probability density function model to connect cloud cover and the distribution of relative humidity, we argue that much of the enhancement is consistent with aerosol hygroscopic growth in the humid environment surrounding clouds. Consideration of these cloud-dependent τ effects will facilitate understanding aerosol-cloud interactions and reduce the uncertainty in estimates of aerosol radiative forcing by global climate models.

Citation: Chand, D., R. Wood, S. J. Ghan, M. Wang, M. Ovchinnikov, P. J. Rasch, S. Miller, B. Schichtel, and T. Moore (2012), Aerosol optical depth increase in partly cloudy conditions, *J. Geophys. Res.*, 117, D17207, doi:10.1029/2012JD017894.

1. Introduction

[2] The indirect effects of aerosol on clouds are among the most important yet least understood processes associated with climate change. Satellite observations suggest that complex interactions occur between coexisting cloud and aerosol layers [Tanré et al., 1997; Ignatov et al., 2005; Kaufman et al., 2005; Loeb and Manalo-Smith, 2005; Matheson et al., 2005; Loeb and Schuster, 2008]. Observations of aerosol optical depth (AOD or τ) from different satellites have been used for model evaluation and for examining aerosol effects on air quality and

climate [Al-Saadi et al., 2005; Quaas et al., 2006; Remer and Kaufman, 2006; Chand et al., 2009; Christopher and Gupta, 2010]. Among the contemporary satellite observing systems, the Moderate-Resolution Imaging Spectrometers (MODIS) on the National Aeronautics and Space Administration (NASA) Terra and Aqua spacecrafts provide perhaps the most comprehensive multispectral record of τ and clouds. One of the primary objectives of MODIS is to provide observations of global aerosol distributions for assessment of their impact on Earth's radiation budget and role in climate change. MODIS 500 m pixels are processed to provide aerosol products at $10 \times 10 \text{ km}^2$ resolution, which is further aggregated to provide gridded global data products at $1^\circ \times 1^\circ$ resolution [Remer and Kaufman, 2006]. Remer et al. [2005] provided global validation that MODIS is comparable to ground-based AERONET observations over both land and oceans.

[3] Solar reflectance is the principal measurement for most of the satellite-based retrievals of aerosol optical properties, specifically for MODIS, over land and oceans. The presence of strongly reflecting clouds represents a major challenge for resolving the relatively weak reflective signals of the more tenuous aerosol layers [Ackerman et al., 1998; Martins et al., 2002]. To overcome these limitations, the MODIS τ retrieval considers only cloud-free pixels; using a sophisticated cloud screen as a preprocessing step [Ackerman et al., 1998; Martins

¹Atmospheric Science and Global Change Division, Pacific Northwest National Laboratory, Richland, Washington, USA.

²Department of Atmospheric Science, University of Washington, Seattle, Washington, USA.

³Cooperative Institute for Research in the Atmosphere, Colorado State University, Fort Collins, Colorado, USA.

⁴Air Resources Division, National Park Service, Fort Collins, Colorado, USA.

⁵Western Regional Air Partnership, Western Governors' Association, Fort Collins, Colorado, USA.

Corresponding author: D. Chand, Atmospheric Science and Global Change Division, Pacific Northwest National Laboratory, Richland, WA 99352, USA. (duli.chand@pnl.gov)

et al., 2002, *Remer et al.*, 2005]. *Ackerman et al.* [1998] provided tests used in the aerosol algorithm's cloud screening, which is described in the *Martins et al.* [2002]. After cloud screening, the MODIS aerosol processing algorithm further reduces cloud contamination and other biases (for example cloud shadows) by excluding both the darkest and brightest 25% of cloud-free pixels in each $10 \times 10 \text{ km}^2$ size area [*Remer et al.*, 2005]. The best (i.e., cloud free and glint free) pixels are averaged, for a 10 km resolution to improve the signal-to-noise ratio [*Remer et al.*, 2005]. In order to screen out cloudy pixels, the MODIS aerosol-retrieving algorithm uses a 3×3 standard deviation (STD) screening test [*Martins et al.*, 2002]. If the STD of reflectance 0.55 nm at a spatial resolution of 500 m is greater than 0.0025, that center pixel of the box is identified as cloudy.

[4] Though great attempts are made to retrieve aerosol properties only from the clear sky pixels at 500 m resolution in partially cloudy conditions, the effect of the clouds over these clear sky pixels is intangible and may significantly influence the aerosol estimates in several ways. The factors impacting both clouds and aerosol retrievals can be due to uptake of water vapor at various stages and scales [*Feingold and Morley*, 2003; *McComiskey and Feingold*, 2012], decayed or evaporated clouds, so-called 'hesitant clouds'—pockets of high humidity that oscillate near saturation [*Koren et al.*, 2008], and three-dimensional cloud scattering effects [*Kaufman et al.*, 2005; *Remer and Kaufman*, 2006; *Mauger and Norris*, 2007; *Loeb and Schuster*, 2008; *Várnai and Marshak*, 2009; *Christopher and Gupta*, 2010]. *Kaufman et al.* [2005] used MODIS and AERONET observations to estimate an enhancement of 0.025 in τ in the vicinity of cirrus and water clouds compared with that far away from clouds at 550 nm. In another similar study, *Zhang et al.* [2005] estimated that clouds increase τ by 10–20%. In two separate studies, *Loeb and Schuster* [2008] and *Mauger and Norris* [2007] pointed to the importance of meteorology (humidity and wind speed) in controlling the τ . *Várnai and Marshak* [2009, 2011] found that brightness of clear sky systematically increases near clouds and that clouds are surrounded by a clear sky transition zone of rapidly changing aerosol optical properties and particle size. In a LIDAR study *Tackett and Di Girolamo* [2009] showed that aerosol properties such as backscatter and color ratio are enhanced adjacent to cloud edge as far as 3 km, particularly near cloud top and cloud base. *Twohy et al.* [2009] demonstrated the effect of changes in relative humidity on aerosol as far as 20 km from clouds. In a similar study *Bar-Or et al.* [2010] found the increase in aerosol optical depth as far as 30 km from the transition zone. Models have been used to quantify the different effects on the AOD - cloud cover relationship found in MODIS and other satellites [*Myhre et al.*, 2007; *Quaas et al.*, 2010].

[5] While most of these studies demonstrate τ enhancements in partly cloudy conditions, none of these studies have explored the effects at large spatial and temporal scales to attempt to understand the large scale behavior of the enhancement. In this study we investigate absolute and relative increases in τ in the presence of clouds using satellite observations. We then employ a simple analytical model to link the aerosol hygroscopic growth with the cloud fraction, and based on the results from this model we argue that much of the observed enhancement can be attributed to

the aerosol hygroscopic growth in the humid environment surrounding clouds. We begin with a summary of observations and methods, followed by presentation of results and conclusions.

2. Observations and Methods

2.1. Satellite Observations

[6] We use aerosol optical depth (τ or AOD) and total cloud fraction (CF) observations from Moderate Resolution Imaging Spectrometer (MODIS) Terra satellite using MOD04_L2_051-version data. Daily global aerosol optical depth observations at $10 \times 10 \text{ km}^2$ resolution are analyzed for the period 2000–2010. These data correspond to about 10:30 A.M. local time. The cloud fraction in aerosol pixels ($10 \times 10 \text{ km}^2$) used here is from aerosol retrievals which are estimated from high resolution ($500 \text{ m} \times 500 \text{ m}$) sub-pixels [*Remer et al.*, 2005; *Levy et al.*, 2009]. The quality assurance flags are used to select and screen the best data. Best quality product and retrieval processing flags over Ocean (usefulness flag = 1 and confidence flag = 3) are used in this analysis. The MODIS aerosol retrievals collocated with AERONET measurements confirm that one standard deviation of MODIS optical thickness retrievals fall within the predicted uncertainty of $0.03 \pm 0.05\tau$ over the oceans [*Remer et al.*, 2005]. As aerosol retrievals over water are more accurate than land [*Remer et al.*, 2005], we restrict our analysis to the oceanic regions only. The retrieval of aerosol is limited over higher latitudes due to low sunlight and reflective snow covered surfaces, so most of the MODIS aerosol observations used here are confined between 70S and 70N. The τ retrievals are grouped by the CF of each $10 \times 10 \text{ km}^2$ pixel, and we primarily focus on the differences between the mean τ values for $0.8 < \text{CF} < 0.9$ and $0.1 < \text{CF} < 0.2$, here termed $\tau_{\text{CF}0.85}$ and $\tau_{\text{CF}0.15}$, respectively. Very high or low cloud fractions (i.e., $\text{CF} = 0.0\text{--}0.1$ or $0.9\text{--}1.0$) are excluded since the number of $10 \times 10 \text{ km}^2$ data pixels for these conditions are low.

[7] The absolute enhancement or increase in aerosol optical depth is defined as $\Delta\tau = \tau_{\text{CF}0.85} - \tau_{\text{CF}0.15}$. A normalized, or relative, increase in aerosol optical depth is defined as ε ($\varepsilon = \Delta\tau/\tau_{\text{CF}0.15}$). This enhancement in ε corresponds to relative enhancement in cloudy conditions ($\text{CF} = 0.8\text{--}0.9$) compared with relatively clear conditions ($\text{CF} = 0.1\text{--}0.2$). Both $\Delta\tau$ and ε are gridded to produce near-global maps at $2.5^\circ \times 2.5^\circ$ resolution for four seasons. To get statistically robust aerosol optical depth in each $2.5^\circ \times 2.5^\circ$ grid, we considered only those grids which have at least 30 or more $10 \times 10 \text{ km}^2$ data points for the selected cloud fraction calculation. Generally, >90% of the total $10 \times 10 \text{ km}^2$ data points averaged in each $2.5^\circ \times 2.5^\circ$ grid are more than 500 for any given season and selected cloudy condition.

2.2. Gaussian PDF Model

[8] We also use a Gaussian probability density function (PDF) approach to estimate the τ enhancement as a function of cloud fraction, assuming that only hygroscopic aerosol growth is important for determining aerosol optical depth enhancement. The physical basis is that the spatial distribution of relative humidity (RH) shifts to higher values in regions with a greater fractional cloud cover, and so the

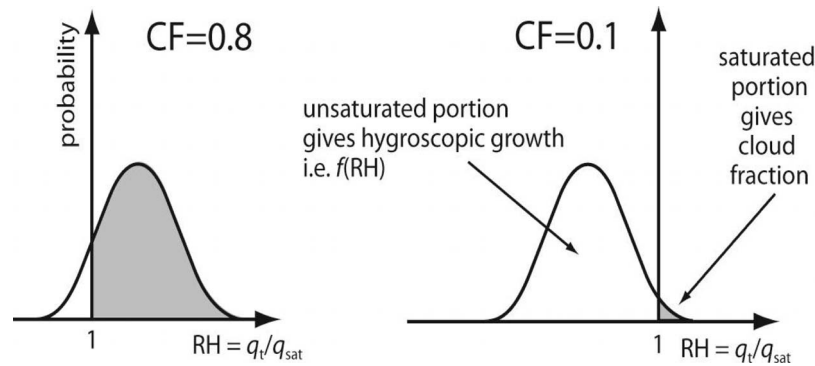


Figure 1. Idealized relative humidity probability density functions demonstrating the relationship between the spatial distribution of relative humidity $p(RH)$ and cloud fraction (CF) as per equations (1) and (2).

mean RH for clear sky regions between clouds is greater (Figure 1). This type of approach actually forms the basis for many statistical cloud schemes used in large scale numerical models, and was first introduced by *Sommeria and Deardorff* [1977] and *Mellor* [1977]. To quantify this hygroscopic enhancement of light scattering for the clear atmospheric columns using PDF approach, we assume the following:

[9] 1. The relative humidity PDF, $p(RH)$, is Gaussian at all levels with a standard deviation that is constant with height and a mean that increases linearly from an assumed value of 80% at the surface to some specified maximum RH at the top, h of the marine boundary layer (MBL). This specified maximum is varied to give variations in hygroscopic growth and cloud cover. No hygroscopic growth is assumed above this level. The choice of 80% for the mean surface RH is in good agreement with observations over much of the global ocean [e.g., *Wood and Bretherton*, 2006].

[10] 2. The cloud fraction is determined as the saturated part of the RH PDF ($RH > 100\%$) at all levels (Figure 1), i.e.,

$$CF = \int_1^{\infty} p(RH) dRH. \quad (1)$$

It is the column maximum cloud fraction that is important for the projected cloud fraction as seen from space and this is (by construction) most of the time at the top of the MBL.

[11] 3. The relative AOD enhancement ε is a fractional enhancement over that for dry aerosol. We assume that dry aerosol extinction β_{dry} is independent of altitude in the MBL, and that the dry aerosol optical depth is independent of cloud cover in a given region. Although scavenging by precipitation from clouds might violate this assumption in model (equation (1)), here we are trying to establish how much the humidity effect alone might contribute. The wet scavenging below clouds has minimum impacts on the present study as our focus is to deal with clear-sky AOD - albeit in cloudy versus less cloudy skies. The aerosol extinction including hygroscopic growth β is estimated as a function of height using the clear sky part ($RH < 100\%$) of the RH PDF, i.e.,

$$\beta = \beta_{dry} \int_0^1 p(RH) f(RH) dRH \quad (2)$$

where $f(RH)$ is the hygroscopic growth factor for aerosol extinction and β_{dry} is the dry aerosol extinction. We then integrate β over height (surface to h), with RH prescribed as a function of height as described in point 1 above, to get a column aerosol optical depth, which can be compared with the dry aerosol optical depth $\tau_{dry} = \beta_{dry}h$. We take $f(RH)$ appropriate for sulfate aerosol from *Kiehl et al.* [2000], namely

$$f(RH) = \exp\left(-1 - \frac{0.6}{RH - 1.2} - \frac{0.75}{RH - 1.5}\right). \quad (3)$$

[12] The growth factor for sea-salt is somewhat higher, but those for pollution aerosol are generally somewhat lower, so our choice represents a compromise but maintains simplicity. For any assumed form and width of $p(RH)$, there is a parametric relationship between AOD and CF through equations (1) and (2). This relationship is a function of the assumed form of $p(RH)$ and the assumed mean and variance of surface RH. The assumptions that $p(RH)$ is Gaussian with a fixed standard deviation, and that the mean surface RH is fixed, result in a unique relationship between τ and CF that depends only upon the assumed PDF width. The PDF width is scale dependent and in general is not well known. However, *Wood et al.* [2002] compiled aircraft estimates of the standard deviation of humidity in the environment of low clouds as a function of length scale. These results suggest that the standard deviation of RH (σ_{RH}) is typically in the range 2–5% (0.02–0.05) at the 10 km scale for marine boundary layer cloud environments. To compare with the MODIS aerosol optical depth observations, we determine the difference in optical depth $\Delta\tau$ between $CF = 0.85$ and that for $CF = 0.15$.

[13] In the MODIS AOD retrievals, the clear-sky pixels in each $10 \times 10 \text{ km}^2$ region used to determine the AOD are additionally screened to remove potentially cloud contaminated pixels. This is carried out, as described in *Remer et al.* [2005], using a two-pronged approach. First, a 3×3 pixel variability mask is used to remove clear pixels immediately adjacent to clouds. Second, the 25% brightest and darkest cloud-free pixels in each $10 \times 10 \text{ km}^2$ are removed from the pixels used to derive aerosol properties to further reduce the impact of cloud contamination and cloud shadows. The combined effect of these screening approaches will likely be

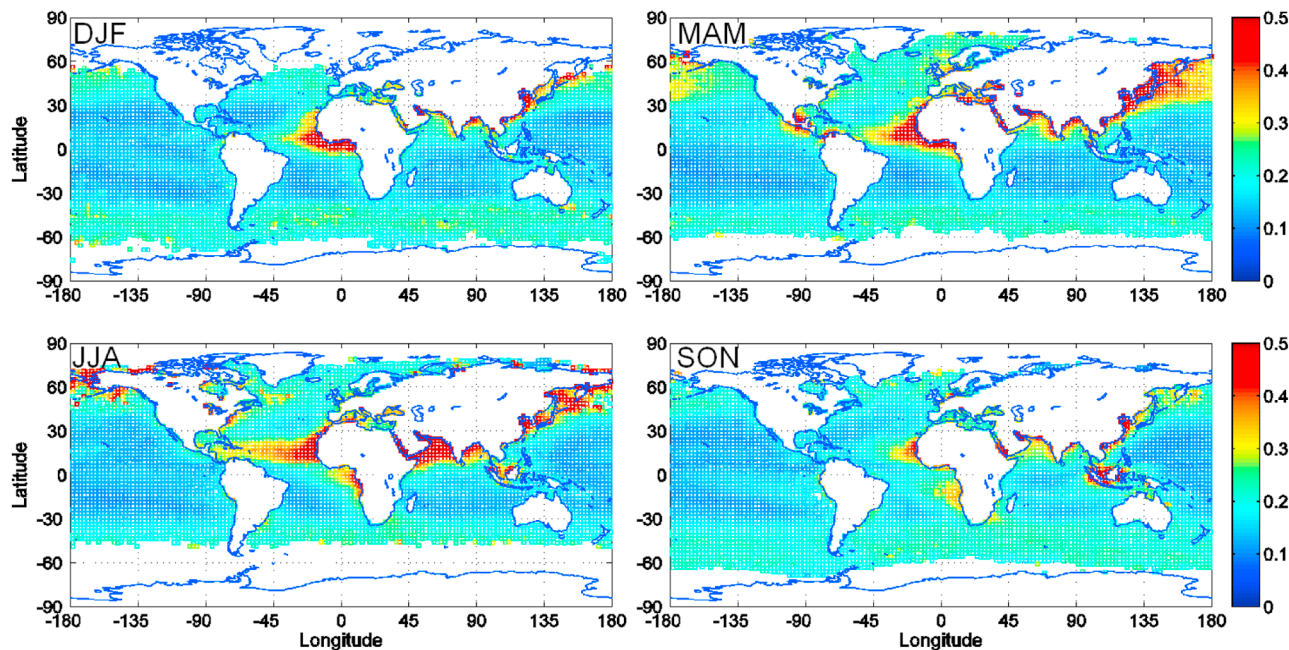


Figure 2. Climatology of seasonal aerosol optical depth ($\tau_{CF0.15}$) from MODIS Terra observations at cloud fraction 0.1–0.2. First letter of each month is used to label the seasons (DJF is for Dec-Jan-Feb). Color bars show the magnitude of τ .

to exclude some clear sky pixels with high humidity, since these are typically found close to clouds. While it is not possible to reproduce this screening with the output from the Gaussian PDF model, we conducted tests to examine the potential impact of additional screening upon the model AOD enhancement. To do this, we conducted a sensitivity test where we removed 25% of clear columns from the model with the greatest hygroscopic growth. Somewhat surprisingly, we find that the growth-restricted mean AOD is only reduced by about 5–10% from that using all the clear columns in the model. The discrepancies are largest when the assumed width of the Gaussian PDF is widest. This is expected because it is the nonlinearity in the $f(\text{RH})$ versus RH curve that introduces the difference. The reason why the difference is not more marked is because the distribution of RH is actually quite narrow ($\sigma_{\text{RH}} = 0.02\text{--}0.05$ is assumed here, see previous paragraph). Further, the AOD reduction is not actually a strong function of cloud fraction, so that the relative enhancement in AOD ($\epsilon = [\tau_{CF0.85} - \tau_{CF0.15}] / \tau_{CF0.15}$) is changed by no more than 3% by restricting the columns with the greatest hygroscopic growth. Because the modeled enhancement $\Delta\tau$ is much larger (15–30%), we believe that our approach of including all clear columns does not introduce a marked bias into the comparisons with the MODIS data.

3. Results and Discussion

[14] Figure 2 shows the seasonal global climatology of aerosols optical depth $\tau_{CF0.15}$ at cloud fraction from 0.10 to 0.20. Higher aerosol optical depth ($\tau_{CF0.15} > 0.5$) is observed in downwind of source regions over Africa and Asia, and moderate levels ($\tau_{CF0.15} \sim 0.25$) over the midlatitude in all the seasons. Lowest aerosol optical depths ($\tau_{CF0.15} \sim 0.1$)

are observed in remote marine environments and also over the intertropical convergence zone (ITCZ). Figure 3 shows the seasonal variation in the absolute aerosol optical depth enhancement, $\Delta\tau$. Large enhancement is observed near the continental source regions, specifically downwind of Asia and Africa, and also during the spring seasons of both hemispheres. A larger enhancement in AOD is observed in northern hemispheric spring (MAM) than the southern hemispheric spring (SON). The global median increase in $\Delta\tau$ is 0.044 (Table 1), and the maximum is 0.24 over the oceans near the aerosol source regions over Africa and Asia. The large spatial variations in $\Delta\tau$ are not likely related to variations in cloud fraction since we used the clear sky pixels from partially cloudy conditions by selecting samples of two narrow cloud cover ranges. Smaller values of $\Delta\tau$ are observed near ITCZ and midlatitudes. The higher $\Delta\tau$ near source regions, and the spatial gradients in $\Delta\tau$ at global scale indicate that the enhancement is likely related to some inherent property of aerosol, like hygroscopicity or burden of hygroscopic aerosol in the vicinity of clouds. We postulate that the effect of clouds adjacent to the satellite field of view humidifies the aerosol in the clear sky twilight zone, and this humidification increases with cloud fraction within the $10 \times 10 \text{ km}^2$ pixel. In other words, as the cloud fraction increases within the scene, the potential for clear sky AOD enhancement in each pixel in proximity of the broken clouds increases in MODIS aerosol products.

[15] The observed global mean enhancement $\Delta\tau$ is a factor of three higher than the *Kaufman et al.* [2005] estimated AOD increase (0.015) as a result of contamination from cirrus clouds, and is a factor of two higher than the *Kaufman et al.* [2005] when accounting for cirrus contamination and aerosol growth together. Though *Kaufman et al.* [2005] indicated that cirrus contamination plays a bigger

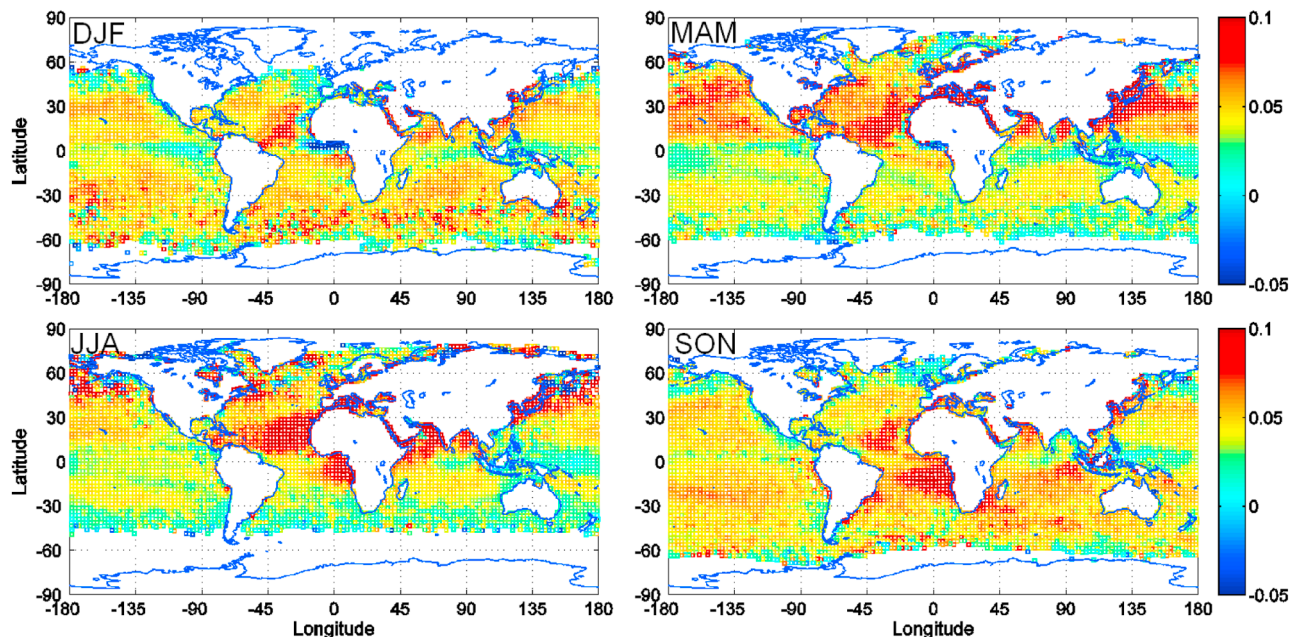


Figure 3. Climatology of seasonal enhancement in aerosol optical depth ($\Delta\tau = \tau_{CF0.85} - \tau_{CF0.15}$) from MODIS Terra observations. First letter of each month is used to label the seasons (DJF is for Dec-Jan-Feb). Color bar shows the magnitude of $\Delta\tau$.

role than hygroscopic growth, the large enhancement in AOD near source regions and lower enhancement over the ITCZ in our analysis highlight the role of hygroscopicity and aerosol washout, respectively, which we will discuss in more detail in the following section.

[16] Variations in relative enhancement $\varepsilon = \Delta\tau/\tau_{CF0.15}$ are much less seasonal than those in $\Delta\tau$, (Figure 4), are approximately zonally symmetric and are not strongly dependent upon longitude (Figure 5). For any given season, ε peaks at the subtropical latitudes ($15\text{--}35^\circ$), where values of 0.25–0.35 are common (Figures 4 and 5). Smaller values of ε (0.15 to 0.25) are found in the midlatitudes (Figure 5). Unlike the absolute enhancement $\Delta\tau$ shown in Figure 3, the relative enhancement ε does not depend strongly upon the absolute aerosol loading. In very few locations, particularly tropical locations in the ITCZ with strong precipitation, ε is observed to be negative. We suspect that the negative ε may result from scavenging of the aerosol by frequent convective precipitation. However, regions with negative ε constitute less than 2% of the oceanic area. Thus, as a result of high RH, the presence of broken clouds enhances the aerosol optical depth in cloud free area over most of the oceanic areas.

[17] We note that the subtropical latitudes where ε is greatest contain very limited amounts of high cloud. Over the oceans, much of the aerosol is located at low levels and particularly within the marine boundary layer with some exceptions found in biomass and dust aerosols layers transported from Africa over the eastern Atlantic Ocean. In the aerosol product used in this study it is not possible to distinguish between high and low clouds, and so we cannot separate our analysis by cloud type. We might expect hygroscopic growth of aerosol to be largely confined to the clouds in the marine boundary layer where the aerosol

primarily resides. It seems reasonable to suggest that in regions containing high clouds the aerosol would largely be at a different level from the location of the clouds, and would therefore not be strongly enhanced by hygroscopic growth. Thus, regions containing a large fraction of high clouds might be reducing the strength of the apparent enhancements due to hygroscopic growth because these data are necessarily included in our analysis.

[18] Figure 6 shows a comparison of hygroscopic enhancements of clear sky aerosol optical depth based on the Gaussian PDF model (described in section 2.2) with the enhancement from MODIS observations. We show this as a function of the upper value of cloud fraction used to determine ε , i.e., $\varepsilon_{CF} = (\tau_{CF} - \tau_{CF0.15})/\tau_{CF0.15}$. The curves represent different plausible values of the free parameters, which are the standard deviation of the Gaussian RH PDF and the mean surface RH. The Gaussian PDF model enhancements at a cloud fraction of 0.85 are of a similar magnitude to observed enhancements shown in Figures 4 and 5. For a given cloud fraction, the relative enhancement is an increasing function of the assumed RH standard deviation. This occurs because the broader RH PDF is more strongly affected by the nonlinearity

Table 1. Seasonal Statistics of Absolute and Relative Enhancements in AOD Estimated From the 11 Years of MODIS Terra Observations Used in Figures 3 and 4

Season	Absolute Enhancement, $\Delta\tau$			Relative Enhancement, ε		
	25th%	50th%	75th%	25th%	50th%	75th%
DJF	0.035	0.045	0.055	0.18	0.26	0.34
MAM	0.031	0.042	0.057	0.16	0.24	0.32
JJA	0.030	0.040	0.055	0.16	0.25	0.32
SON	0.037	0.047	0.055	0.19	0.26	0.34
Annual	0.033	0.044	0.055	0.17	0.25	0.33

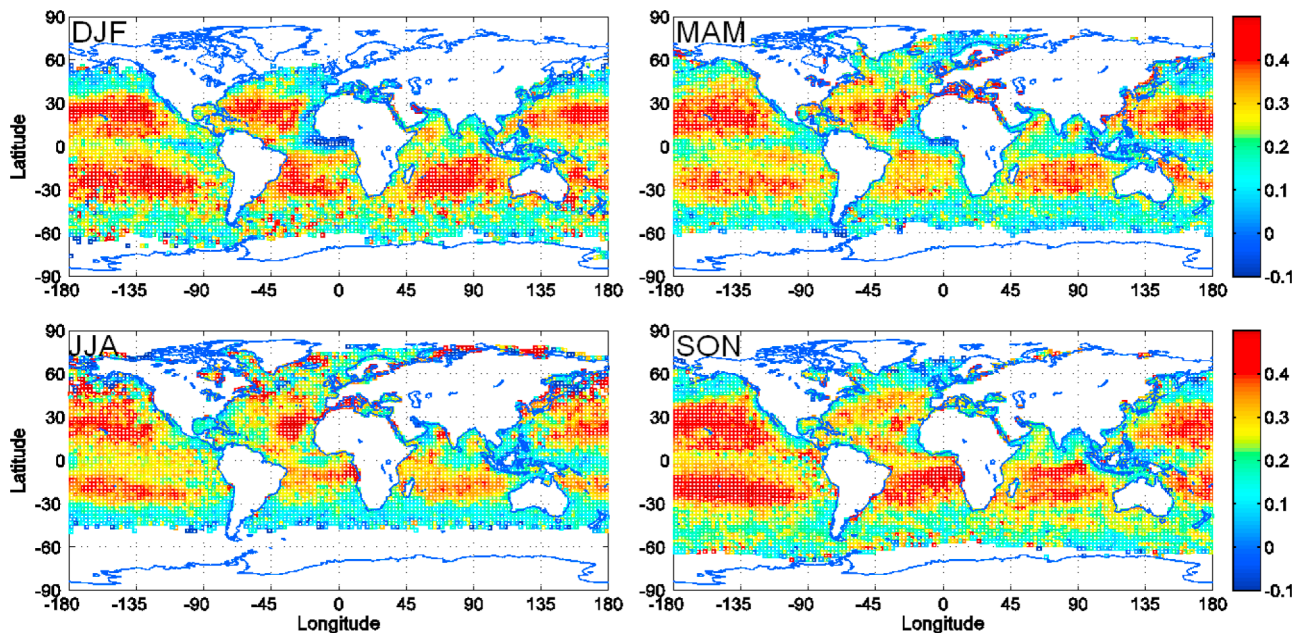


Figure 4. Same as Figure 3 but for the relative enhancement, $\epsilon = \Delta\tau/\tau_{CF0.15}$.

in $f(RH)$ (equation (3) above) than a narrow RH PDF, which increases the difference in hygroscopic growth between more and less cloudy boxes. The increase in ϵ_{CF} with CF is quasi-linear in the model, whereas the observations show a more nonlinear behavior, with stronger increases at high cloud fraction. This may reflect changes in the observed PDF width or skewness with cloud fraction, but may be caused by factors that the model cannot address, such as cloud contamination. Sensitivity studies where the mean RH is assumed to be constant with height rather than linearly increasing (see section 2.2) leads to some qualitative differences in the ϵ_{CF} curves, but the essential behavior of ϵ_{CF} increasing with CF, and the approximate magnitude of the enhancements, are unchanged.

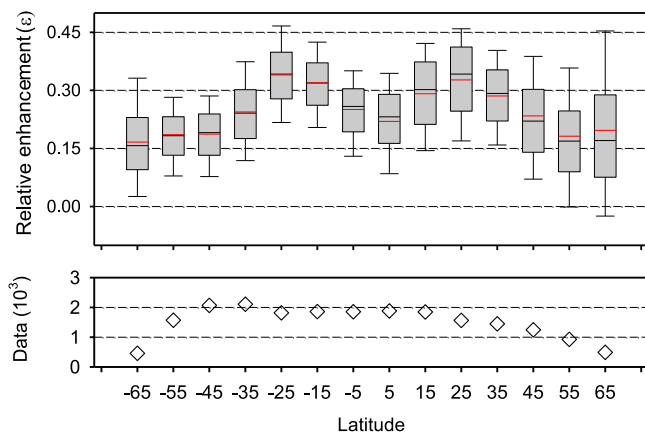


Figure 5. (top) Annual variation of the relative aerosol optical depth enhancement (ϵ) with latitude. The solid black line (starting from lower side of box plot) of box plot are 5, 25, 50, 75 and 95 percentiles. The red line in each box is mean of the (ϵ). (bottom) The number of data points (in thousands) for each 10 degree latitudinal bin.

[19] As discussed above, we do not expect to see enhancements in τ for aerosol within clear sky regions between high clouds. Because cloud height information is not provided in the Level 2 aerosol data used here, we weight the mean model enhancements by $1 - CF_{high}$ where CF_{high} is the annual mean non-liquid cloud cover taken from MODIS Level 3 cloud products, and plot these as a function of latitude (Figure 7). Although there is discrepancy in the mean values, the weighted model enhancements show similar latitudinal variability to the observations, suggesting that

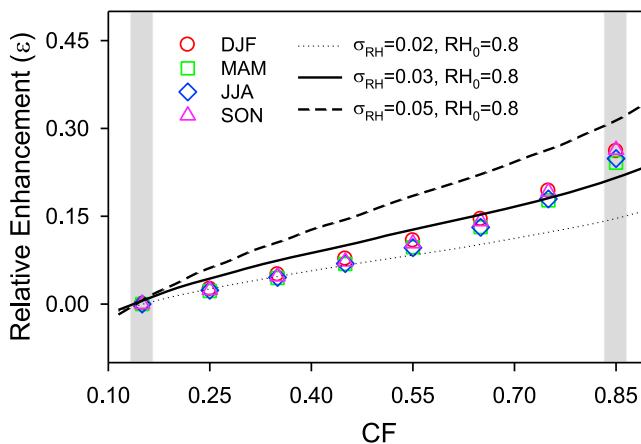


Figure 6. Enhancement in clear sky AOD for varying cloud cover derived from hygroscopic growth of aerosol [Kiehl et al., 2000] for three values of the assumed RH PDF width ($\sigma_{RH} = 0.02$, dotted line; $\sigma_{RH} = 0.03$, solid thick line; $\sigma_{RH} = 0.05$, dashed line) and at values of the assumed mean surface RH (80%) using the statistical model. The symbols are seasonal enhancement in AOD (ϵ) with CF from 11 years of MODIS Terra observations for DJF (circles), MAM (squares), JJA (diamonds), and SON (triangles).

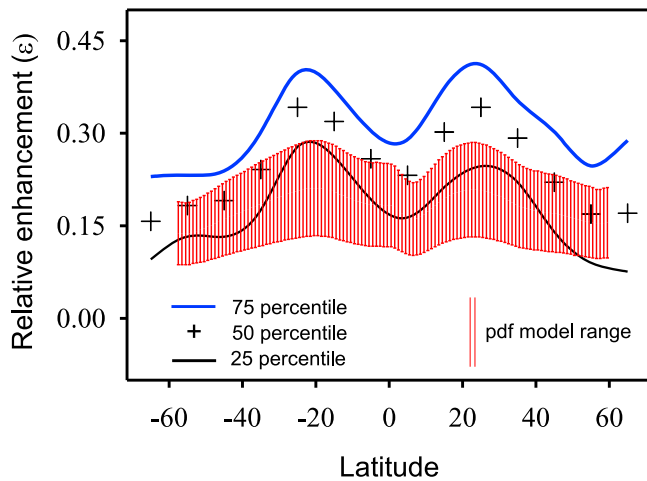


Figure 7. Variation of the relative aerosol optical depth enhancement (ε) from low level clouds with latitude using statistical model based on equations (1)–(3) and weighted with $1-CF_{\text{high}}$ (red lines, see the text for more explanation). The shaded red area with vertical lines show the range of the ε from the PDF model with the lower and upper limits corresponding to the plausible range of Gaussian PDF width $0.02 < \sigma_{\text{RH}} < 0.05$. Without cloud fraction weighting the range for model ε would be 0.15–0.32 with no latitudinal variation. The annual relative enhancement (ε) from MODIS observations used in Figure 4 is also shown here for inter-comparison purpose (black and blue lines). The thick blue line, plus sign and thin black line are 75th, 50th and 25th percentiles of MODIS observed ε , respectively.

the meridional pattern of τ enhancement globally is broadly consistent with aerosol hygroscopic growth. Assuming an average global oceanic CF of 0.51, the estimated global ε is 0.09.

[20] The agreement between the simple Gaussian hygroscopic growth model and the observations does not definitively prove that hygroscopic growth is the dominant reason for the observed τ enhancement near clouds. Though the PDF model captures key aspects of the spatial pattern in ε , the observed zonal mean values are somewhat higher, possibly due to cloud contamination, additional effects like 3D light scattering effects [Várnai and Marshak, 2009], and possible meteorological correlations between dry aerosol and clouds [Matheson et al., 2006; George and Wood, 2010]. The hygroscopic growth model cannot explain the very lowest values observed in the ITCZ and in the midlatitude storm tracks. Cloud masking by high clouds in these regions, although significant, only reduces the weighted model ε values by 0.12. So scavenging effects in cloudy regions are likely to play some (as yet unknown) role in the global distribution of ε . However, the results are consistent with a GCM model study [Quaas et al., 2010] that found aerosol hygroscopic growth to be the dominant factor controlling the global relationship between cloud cover and aerosol optical thickness.

[21] The absolute and relative enhancements in τ at large spatial and temporal scales can be useful to understand the large-scale influence of clouds on aerosol and the impact of clouds on the aerosol direct radiative forcing. Examining

enhancements at the regional spatial scale and seasonal timescale should help constrain global aerosol models and better quantify the aerosol direct radiative forcing. As our PDF model is unable to explain the negative ε values observed in the ITCZ and in the midlatitude storm tracks, extending this work with a GCM model will be helpful. Further, observations from satellites [e.g., Quaas, 2012] can now be used to determine the humidity PDF widths that have been assumed in this study. In future work it would be useful to use observations from other satellites to better constrain our model of the aerosol hygroscopic growth and examine how it affects the regional distribution of AOD enhancement.

4. Summary

[22] Eleven years of daily MODIS Terra observations along with a simple diagnostic model are used to estimate the enhancement in τ in clear sky zones under partially cloudy conditions at global scale. The summary of results is as follows.

[23] 1. The enhancement of aerosol optical depth as cloud cover increases is quantitatively consistent with hygroscopic growth in humid regions in the vicinity of clouds. The absolute enhancement $\Delta\tau$ (0.044) is about 25% of the global aerosol optical depth at total cloud fraction of 0.85.

[24] 2. The observed relative enhancement ε at global mean cloud fraction of 0.51 is about 0.09.

[25] 3. The increase in τ is higher in the spring season of each hemisphere, particularly the northern hemispheric spring season.

[26] 4. Unlike $\Delta\tau$, the relative enhancement ε is independent of source region and ranges from 0.25 to 0.35 in the subtropics and 0.15–0.25 in the midlatitudes.

[27] 5. The relative enhancement ε shows latitudinal variations with peaks at subtropical latitudes, and has a similar spatial pattern in all seasons. There are some small marine areas (<2% of globe) over ITCZ, showing negative ε , possibly as a result of scavenging the aerosol by rain.

[28] 6. A simple Gaussian PDF model relating the relative humidity in clear sky regions between clouds to the cloud fraction produces enhancements consistent with observations, suggesting that much of the increase in τ can be explained by hygroscopic growth.

[29] **Acknowledgments.** The MODIS data used in this study were acquired as part of NASA's Earth Science Enterprise. PNNL work was supported by the NASA Interdisciplinary Science Program under grant NNX07A156G, the U.S. Department of Energy (DOE), Office of Science, Atmospheric System Research and Earth System Modeling Programs, the DOE Scientific Discovery through Advanced Computing (SciDAC) program, and the DOE Decadal and Regional Climate Prediction using Earth System Models (EaSM) program. UW work was supported by NASA grant NNX10AN78G. We thank three anonymous reviewers and the associate editor for their constructive inputs which have improved the quality of our manuscript.

References

- Ackerman, S. A., K. I. Strabala, W. P. Menzel, R. A. Frey, C. C. Moeller, and L. E. Gumley (1998), Discriminating clear sky from clouds with MODIS, *J. Geophys. Res.*, *103*, 32,141–32,157, doi:10.1029/1998JD200032.
- Al-Saadi, J., et al. (2005), Improving national air quality forecasts with satellite aerosol observations, *Bull. Am. Meteorol. Soc.*, *86*, 1249–1261, doi:10.1175/BAMS-86-9-1249.

- Bar-Or, R. Z., I. Koren, and O. Altaratz (2010), Estimating cloud field coverage using morphological analysis, *Environ. Res. Lett.*, 5(1), 014022, doi:10.1088/1748-9326/5/1/014022.
- Chand, D., R. Wood, T. L. Anderson, S. K. Satheesh, and R. J. Charlson (2009), Satellite-derived direct radiative effect of aerosol dependent on cloud cover, *Nat. Geosci.*, 2, 181–184, doi:10.1038/ngeo437.
- Christopher, S. A., and P. Gupta (2010), Satellite remote sensing of particulate matter air quality: The cloud-cover problem, *J. Air Waste Manage. Assoc.*, 60, 596–602, doi:10.3155/1047-3289.60.5.596.
- Feingold, G., and B. Morley (2003), Aerosol hygroscopic properties as measured by lidar and comparison with in situ measurements, *J. Geophys. Res.*, 108(D11), 4327, doi:10.1029/2002JD002842.
- George, R. C., and R. Wood (2010), Subseasonal variability of low cloud radiative properties over the southeast Pacific Ocean, *Atmos. Chem. Phys.*, 10, 4047–4063, doi:10.5194/acp-10-4047-2010.
- Ignatov, A., et al. (2005), Two MODIS aerosol products over ocean on the Terra and Aqua CERES SSF datasets, *J. Atmos. Sci.*, 62, 1008–1031, doi:10.1175/JAS3383.1.
- Kaufman, Y., et al. (2005), A critical examination of the residual cloud contamination and diurnal sampling effects on MODIS estimates of aerosol over ocean, *IEEE Trans. Geosci. Remote Sens.*, 43, 2886–2897, doi:10.1109/TGRS.2005.858430.
- Kiehl, J. T., T. L. Schneider, P. J. Rasch, M. C. Barth, and J. Wong (2000), Radiative forcing due to sulfate aerosol from simulations with the National Center for Atmospheric Research Community Climate Model, Version 3, *J. Geophys. Res.*, 105, 1441–1457, doi:10.1029/1999JD900495.
- Koren, I., L. Oreopoulos, G. Feingold, L. A. Remer, and O. Altaratz (2008), How small is a small cloud?, *Atmos. Chem. Phys.*, 8, 3855–3864, doi:10.5194/acp-8-3855-2008.
- Levy, R. C., L. A. Remer, D. Tanré, S. Mattoo, and Y. J. Kaufman (2009), Algorithm for remote sensing of tropospheric aerosol over dark targets from MODIS: Collections 005 and 051: Revision 2, *MOD04/MYD04*, NASA Goddard Space Flight Cent., Greenbelt, Md.
- Loeb, N. G., and N. Manalo-Smith (2005), Top-of-atmosphere direct radiative effect of aerosols over global oceans from merged CERES and MODIS observations, *J. Clim.*, 18, 3506–3526.
- Loeb, N. G., and G. L. Schuster (2008), An observational study of the relationship between cloud, aerosol and meteorology in broken low-level cloud conditions, *J. Geophys. Res.*, 113, D14214, doi:10.1029/2007JD009763.
- Martins, J. V., D. Tanré, L. Remer, Y. Kaufman, S. Mattoo, and R. Levy (2002), MODIS cloud screening for remote sensing of aerosol over oceans using spatial variability, *Geophys. Res. Lett.*, 29(12), 8009, doi:10.1029/2001GL013252.
- Matheson, M. A., J. A. Coakley Jr., and W. R. Tahnk (2005), Aerosol and cloud property relationships for summertime stratiform clouds in the northeastern Atlantic from Advanced Very High Resolution Radiometer observations, *J. Geophys. Res.*, 110, D24204, doi:10.1029/2005JD006165.
- Matheson, M. A., J. A. Coakley Jr., and W. R. Tahnk (2006), Multiyear Advanced Very High Resolution Radiometer observations of summertime stratocumulus collocated with aerosol in the northeastern Atlantic, *J. Geophys. Res.*, 111, D15206, doi:10.1029/2005JD006890.
- Mauger, G. S., and J. R. Norris (2007), Meteorological bias in satellite estimates of aerosol-cloud relationships, *Geophys. Res. Lett.*, 34, L16824, doi:10.1029/2007GL029952.
- McComiskey, A., and G. Feingold (2012), The scale problem in quantifying aerosol indirect effects, *Atmos. Chem. Phys.*, 12, 1031–1049, doi:10.5194/acp-12-1031-2012.
- Mellor, G. L. (1977), The Gaussian cloud model relations, *J. Atmos. Sci.*, 34, 356–358, doi:10.1175/1520-0469(1977)034<0356:TGCMR>2.0.CO;2.
- Myhre, G., F. Stordal, M. Johnsrud, Y. J. Kaufman, D. Rosenfeld, T. Storelvmo, J. E. Kristjansson, T. K. Berntsen, A. Myhre, and I. S. A. Isaksen (2007), Aerosol-cloud interaction inferred from MODIS satellite data and global aerosol models, *Atmos. Chem. Phys.*, 7, 3081–3101, doi:10.5194/acp-7-3081-2007.
- Quaas, J. (2012), Evaluating the “critical relative humidity” as a measure of subgrid-scale variability of humidity in general circulation model cloud cover parameterizations using satellite data, *J. Geophys. Res.*, 117, D09208, doi:10.1029/2012JD017495.
- Quaas, J., O. Boucher, and U. Lohmann (2006), Constraining the total aerosol indirect effect in the LMDZ and ECHAM4 GCMs using MODIS satellite data, *Atmos. Chem. Phys.*, 6, 947–955.
- Quaas, J., B. Stevens, P. Stier, and U. Lohmann (2010), Interpreting the cloud cover–aerosol optical depth relationship found in satellite data using a general circulation model, *Atmos. Chem. Phys.*, 10, 6129–6135, doi:10.5194/acp-10-6129-2010.
- Remer, L. A., and Y. J. Kaufman (2006), Aerosol direct radiative effect at the top of the atmosphere over cloud-free ocean derived from four years of MODIS data, *Atmos. Chem. Phys.*, 6, 237–253, doi:10.5194/acp-6-237-2006.
- Remer, L. A., et al. (2005), The MODIS aerosol algorithm, products and validation, *J. Atmos. Sci.*, 62, 947–973, doi:10.1175/JAS3385.1.
- Sommeria, G., and J. W. Deardorff (1977), Subgrid-scale condensation in models of nonprecipitating clouds, *J. Atmos. Sci.*, 34, 344–355, doi:10.1175/1520-0469(1977)034<0344:SSCIMO>2.0.CO;2.
- Tackett, J. L., and L. Di Girolamo (2009), Enhanced aerosol backscatter adjacent to tropical trade wind clouds revealed by satellite-based lidar, *Geophys. Res. Lett.*, 36, L14804, doi:10.1029/2009GL039264.
- Tanré, D., Y. J. Kaufman, M. Herman, and S. Mattoo (1997), Remote sensing of aerosol over oceans from EOS-MODIS, *J. Geophys. Res.*, 102, 16,971–16,988.
- Twohy, C. H., J. A. Coakley Jr., and W. R. Tahnk (2009), Effect of changes in relative humidity on aerosol scattering near clouds, *J. Geophys. Res.*, 114, D05205, doi:10.1029/2008JD010991.
- Várnai, T., and A. Marshak (2009), MODIS observations of enhanced clear sky reflectance near clouds, *Geophys. Res. Lett.*, 36, L06807, doi:10.1029/2008GL037089.
- Várnai, T., and A. Marshak (2011), Global CALIPSO observations of aerosol changes near clouds, *IEEE Geosci. Remote Sens. Lett.*, 8(1), 19–23.
- Wood, R., and C. S. Bretherton (2006), On the relationship between stratiform low cloud cover and lower-tropospheric stability, *J. Clim.*, 19, 6425–6432, doi:10.1175/JCLI3988.1.
- Wood, R., P. R. Field, and W. R. Cotton (2002), Autoconversion rate bias in stratiform boundary layer cloud parameterizations, *Atmos. Res.*, 65, 109–128, doi:10.1016/S0169-8095(02)00071-6.
- Zhang, J., J. S. Reid, and B. N. Holben (2005), An analysis of potential cloud artifacts in MODIS over ocean aerosol optical thickness products, *Geophys. Res. Lett.*, 32, L15803, doi:10.1029/2005GL023254.